
EUV IMAGING SPECTROMETER

Hinode

EIS SOFTWARE NOTE No. 12

Version 1

5 February 2010

STRAY LIGHT

Ignacio Ugarte
Naval Research Laboratory
4555 Overlook Ave SW
Washington, DC 20004
U.S.A.

iugarte@ssd5.nrl.navy.mil

1 Introduction

Stray light is the part of the radiation that impinges the detector following paths that were not originally intended in the optical system. The source can be light scattered by external or internal agents, including dust, imperfections in the optical system, scattering from supporting structures, etc.

In this EIS note, we present a brief analysis of observations during a solar eclipse to show the effects that stray light can have in the observations. The purpose of this note is to make the EIS users aware of this potential contamination effect. As of this version, no correction is provided.

2 Sample dataset: solar eclipse

To measure the stray light component we need to separate it from the direct component. During an eclipse, with no direct light aimed at the detector, any measurement on the EIS detector will be due to the stray contribution.

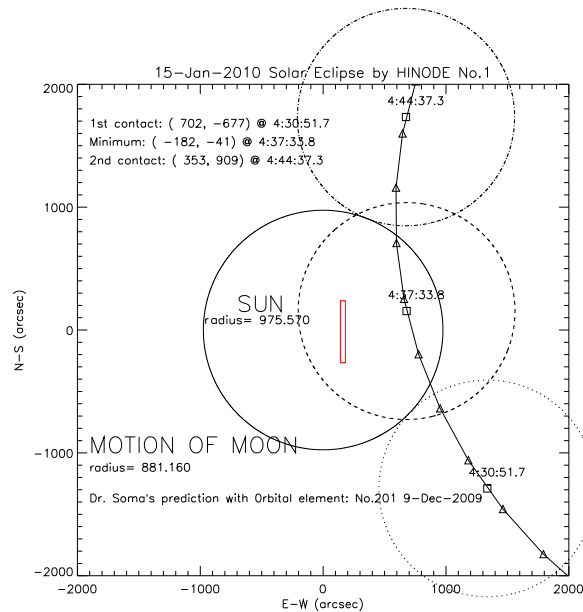


Figure 1: Eclipse on 2010 January 15 when stray light observations were taken. In red the EIS field of view.

We investigated the EIS measurements on the detector during the eclipse that took place on 2010 January 15 (Fig. 1). An specific sequence was run for this purpose (Table 1). It consisted of a set of sit-and-stare 40'' slit images in three spectral windows (Ca XVII 192.82 Å, Fe XII 195.12 Å and He II 256.32 Å) framed by two dark current measurements (REGCAL015), one before and one after. During the dark current measurements the shutter remains closed and therefore no light (stray or direct) should reach the detector. The counts (data numbers, DN) measured with the shutter closed are used as the reference to estimate the stray light component when it is open. We should state that we have used only the dark current exposures with the same integration time (10s) as the observations.

Table 1: Eclipse's observing sequence

File	Study Acronym	Description
eis_l0_20100115_042142.fits	REGCAL015	8 dark exposures, full CCD (exposure times: 1,1,10,10,30,30,60,60s)
eis_l0_20100115_043013.fits	TEST_STUDY	[SNS:10sets][ss:40 ^{''}][wH:512,nWins:3][ExpT(Delay):10.00(0)]
eis_l0_20100115_043213.fits	TEST_STUDY	[SNS:10sets][ss:40 ^{''}][wH:512,nWins:3][ExpT(Delay):10.00(0)]
eis_l0_20100115_043413.fits	TEST_STUDY	[SNS:10sets][ss:40 ^{''}][wH:512,nWins:3][ExpT(Delay):10.00(0)]
eis_l0_20100115_043613.fits	TEST_STUDY	[SNS:10sets][ss:40 ^{''}][wH:512,nWins:3][ExpT(Delay):10.00(0)]
eis_l0_20100115_043812.fits	TEST_STUDY	[SNS:10sets][ss:40 ^{''}][wH:512,nWins:3][ExpT(Delay):10.00(0)]
eis_l0_20100115_044012.fits	TEST_STUDY	[SNS:10sets][ss:40 ^{''}][wH:512,nWins:3][ExpT(Delay):10.00(0)]
eis_l0_20100115_044212.fits	TEST_STUDY	[SNS:10sets][ss:40 ^{''}][wH:512,nWins:3][ExpT(Delay):10.00(0)]
eis_l0_20100115_044512.fits	REGCAL015	8 dark exposures, full CCD (exposure times: 1,1,10,10,30,30,60,60s)

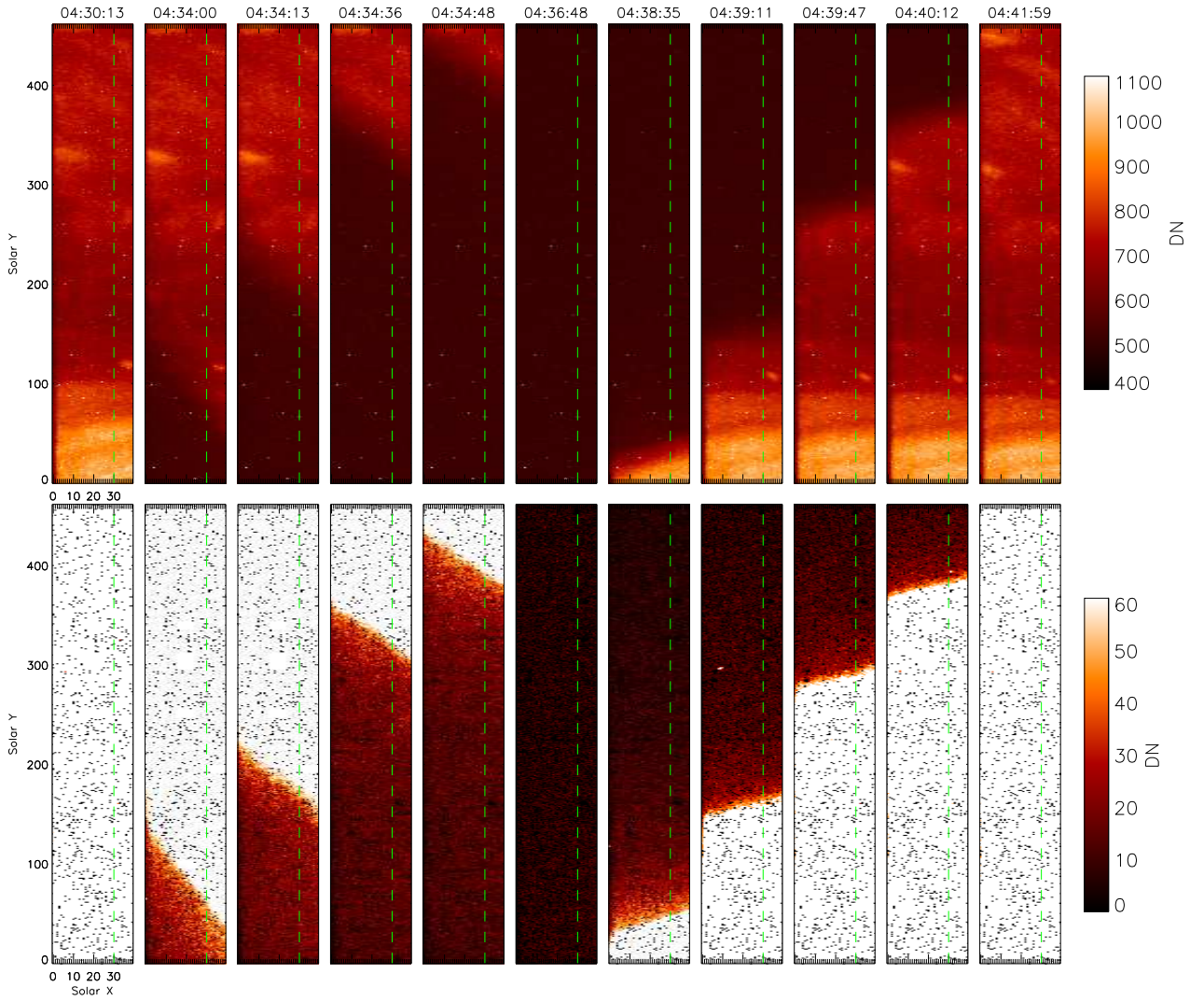


Figure 2: Eclipse sequence as seen in Fe XII 195.12 Å. Top: signal in counts. Bottom: residuals from subtracting the dark current. When comparing to Fig. 1, note that images on the detector are flipped in the E–W direction.

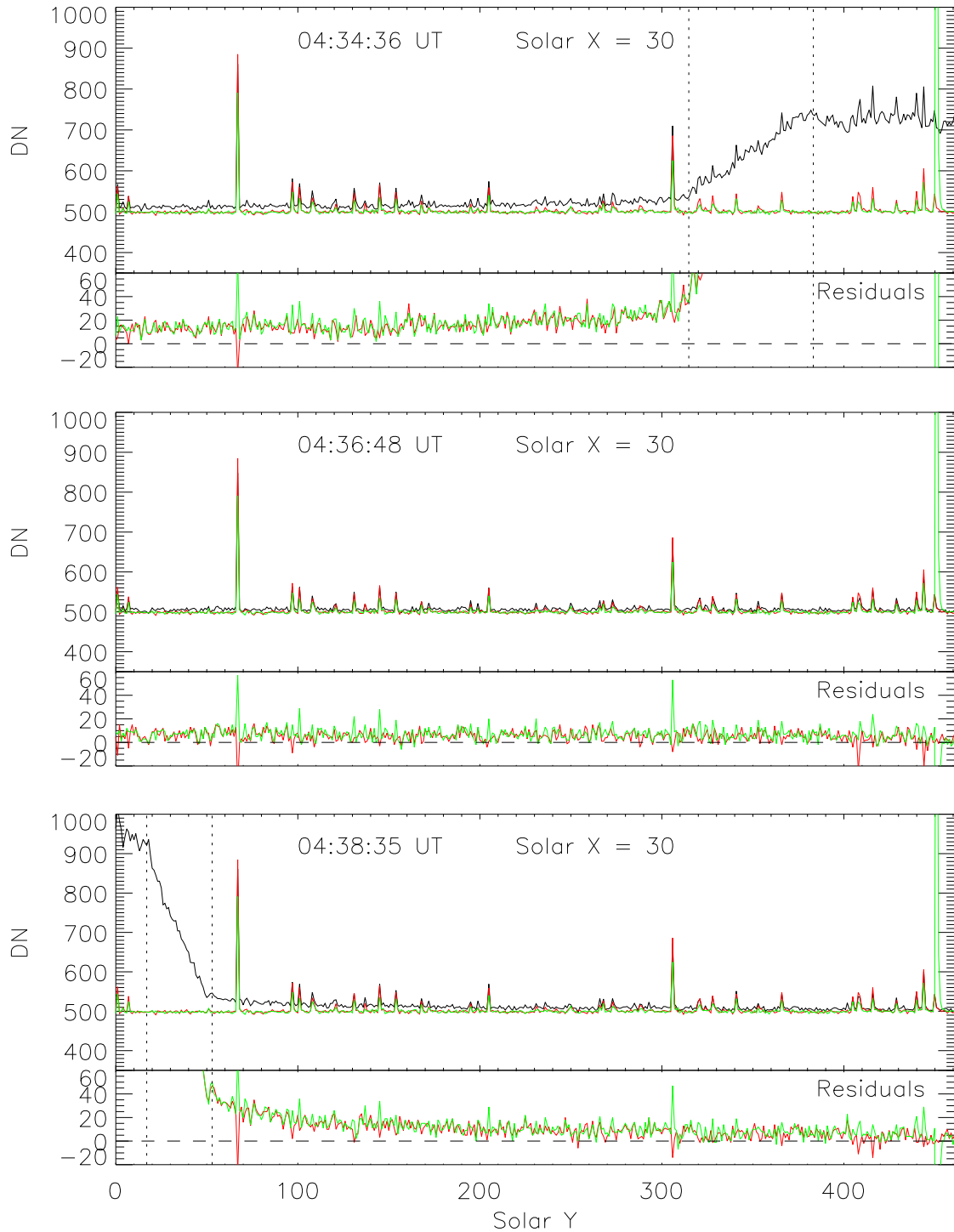


Figure 3: Larger panels: intensity cross-sections along the slit for position 30 in Solar X at three different times during the eclipse. In red and green dark current measurements before and after the sequence. Dotted lines indicate the distance traveled by the Moon during the exposure. The residuals from subtracting the dark current are shown in the smaller panels

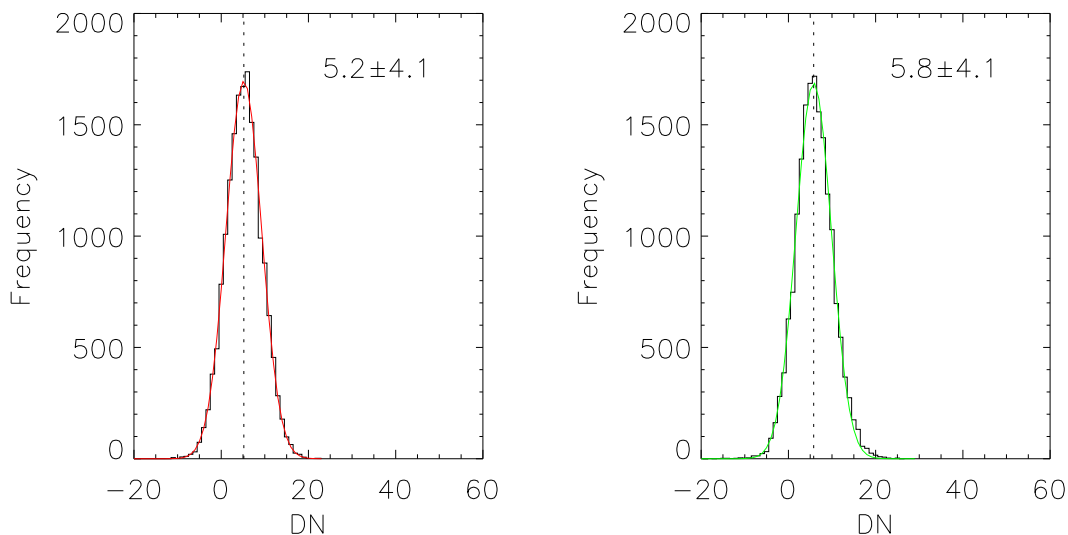


Figure 4: Histograms of residuals from subtracting the two dark current files to exposure 04:36:48 UT (time step 33). The dotted lines indicate the center of the Gaussian fit given also in the legend with the standard deviation error from the Gaussian width.

The top panels in Fig. 2 show a subset of the frames in the eclipse sequence, as seen in Fe XII 195.12 Å. The dark current counts level for this section of the detector is around 500 counts. If we subtract the dark current (04:45 UT file), we obtain the residuals shown in the bottom row, where we have saturated anything above 60 DN. That brings out the signal in the part of the detector that has been occulted by the Moon. Signal there is not due to direct light coming from the Sun, but from light following a stray path. The black dots sprinkled over the field of view are warm and hot pixels.

One obvious thing to note is that there is no sharp transition between the exposed part of the detector and the occulted one. Two are the contributions to this effect: the Moon’s displacement across the field of view and stray light. The Moon is moving while the exposure is being taken (10s) and this results in a gradual occultation of the disk and therefore a gradient in intensity. We have estimated the displacement of the Moon’s leading edge in 6.84 pixels/s and in 3.59 pixels/s for the trailing one (see the Appendix). The exposures are 10s and therefore the intensity of as many as 68 and 36 pixels along the slit suffers attenuation due to the Moon movement.

Fig. 3 shows this in more detail. The intensity along the slit for one Solar X (green dashed line in Fig. 2) at three different times is displayed as a black solid line: Moon’s leading edge in the field of view; full occultation; and trailing edge in the field of view. The red and green lines are dark current counts before and after the occultation respectively. The spikes come from warm and hot pixels and have not been removed to show that we are really looking at the same part of the detector in all three curves. Below each intensity panel, we show a smaller panel with the residuals from subtracting the dark current measurements at each pixel. The dotted lines indicate the separation in pixels between the spatial start of the intensity decay and the end of the estimated distance covered by the Moon’s edge at the velocities described earlier. The intensity decay shows two clearly defined slopes: a steep decrease that coincides with the passage of the Moon while the detector is being exposed and a slower decay from there onwards. The pixels in the latter part of

the detector are, according to this, already fully occulted by the Moon. Therefore the excess of counts has to come from stray light that shouldn't be there.

An exponential fit $A_0 \exp^{-x/A_1} + A_2$ to the gentle slope in the bottom panel (04:38 UT), avoiding spikes, gives an amplitude of $A_0 \approx 25$ counts, $A_1 \approx 78$ pixels and $A_2 \approx 507$ DN. A_0 and A_1 can change for different profiles. They are representative, but are not sufficiently accurate to derive a universally valid correction curve as function of distance to the source. This dataset due to the Moon's rapid displacement is probably not optimal to estimate that sort of correction.

We can, however, estimate the minimum stray light level above the dark current. Fig. 4 shows the histograms of the residuals from subtracting the two dark current exposures to a exposure fully eclipsed (04:36:48 UT, time step 33). It reveals an excess of 5–6 DN over the dark current levels. As no significant differences can be found between the two histograms produced using the two dark current files set at the beginning and end of the observational sequence, 20 minutes apart, we can rule out the time variability of the dark current as responsible for that excess. We can therefore safely conclude that a minimum of 5–6 counts should be expected from stray light in Fe II 195.12 Å. This is when half of the solar disk is eclipsed by the Moon. That is around 2% of the typical counts for that line in the field of view.

A similar analysis was done with He II 256.32 Å and the blended Ca XVII 192.82 Å. The Gaussian fits to the histograms return: -1.2 ± 3.6 DN and 0.8 ± 3.7 DN in the first case, and 2.1 ± 3.9 DN and 2.7 ± 3.9 DN in the second. These numbers are also at the 2% level of the typical counts in each spectral window.

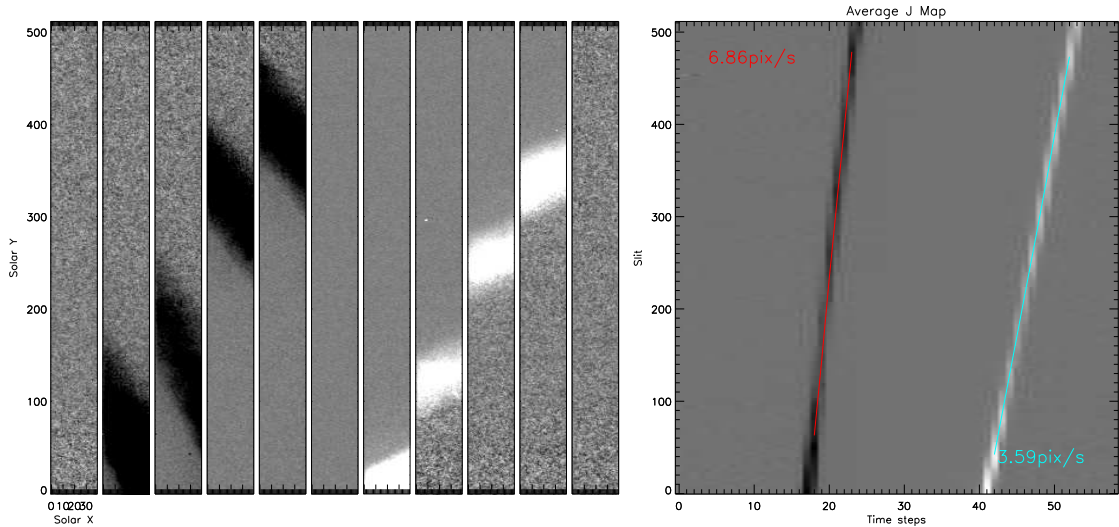


Figure 5: Left panels: running differences from the same frames as shown in Fig 2. Right panel: average J-map of the sequence. J-map represents height versus time. Velocities from the linear fit to the valleys and peaks at each time step are given color coded.

A Moon's occultation speed

The velocity of the Moon's edges crossing the EIS field of view was estimated using running difference images. Fig. 5 shows the running differences for the same frames as Fig. 2. Then a J-map

was constructed by averaging the intensity along the slit for each frame (time step) and sticking them together in sequence (right panel of Fig. 5). The two inclined ridges represent the edges of the Moon crossing the field of view from bottom to top. A linear fit to the central point of the ridges at each time step provides us with the velocity. The values we obtain are 6.86 pixels/s for the leading edge and 3.59 pixels/s for the trailing one.